Study of trapping in Sb_xSe_{1-x} amorphous semiconductors

1994 J. Phys.: Condens. Matter 6 8269

(http://iopscience.iop.org/0953-8984/6/40/017)

J. Phys.: Condens. Matter 6 (1994) 8269–8275. Printed in the UK

Study of trapping in Sb_xSe_{1-x} amorphous semiconductors

V I Mikla, I P Mikhalko and Yu Yu Nagy

Institute of Solid State Physics and Chemistry, Uzhgorod State University, Voloshina St 54, 294000, Ukraine

Received 6 May 1994

Abstract. We investigated the effect of the addition of Sb atoms on the properties of defect states of pure amorphous selenium. The trap levels have been studied by a combination of conventional thermally stimulated depolarization current spectroscopy and time-of-flight measurements. Taken together, these experiments show that Sb introduces a new set of shallow traps for electrons at energies 0.22, 0.34 and 0.45 eV below the conduction band edge, in addition to that existing in pure selenium. At the same time, progressive addition of antimony markedly enhances the deep trapping of holes.

1. Introduction

Chalcogenide glassy semiconductors have a number of superior properties that can be applied to devices [1–3]. Except for optical sensors and electrophotography, however, applications of glassy chalcogenide semiconductors at present are few. This is considered to be because the effects of impurity addition are still not well understood. Hence, the extent to which the optical, photoelectronic and other commercially desirable properties can be varied in this remains a key issue in the study of the above-mentioned class of glassy materials.

Amorphous selenium is a prototypical system whose elemental nature, relative structural simplicity, ambipolarity, high photosensitivity, etc, make it particularly suitable for such a study.

The aim of the present investigation is to study the influence of the addition of Sb atoms on the properties of defect states of amorphous selenium. Recently films of these materials have become of interest for use in data storage, because of their large photostructural transformation [4, 5]. The latter can be explained by local phase transition, stimulated by non-equilibrium carriers captured on the shallow traps [4].

The thermally stimulated conductivity (TSC) is a well known technique for obtaining data on the trapping levels of crystalline semiconductors [6, 7], and the technique has also been applied to amorphous semiconductors [8–10]. One of the main difficulties in observing TSC in amorphous semiconductors is the small magnitude of the TSC currents [11–13]. There are cases in which the TSC measurements yield no peak. We were able to overcome this difficulty by using the analysis of the thermally stimulated depolarization (TSD) current in samples previously polarized by the photoelectret effect. In earlier work [14, 15] we have demonstrated the applicability of the method for obtaining information on the gap states of amorphous semiconductors. We preferred TSD experiments because of the absence of noise due to the voltage source, and strongly reduced influence of the intrinsic conductivity. In order to determine the type of carrier traps involved in TSD, time-of-flight experiments were also performed.

0953-8984/94/408269+07$19.50

2. Experimental details and procedure

2.1. Glass preparation

Binary Sb_xSe_{1-x} ($x \leqslant 0.05$) chalcogenides were prepared by direct reaction of high-purity elements. The glass samples were prepared by mixing the appropriate amount of the constituents Sb and Se. The cleaned silica tubes containing the mixture were evacuated to 10^{-5} Torr and sealed. The contents of the tubes were melted in a furnace and continuously agitated for 10 h to ensure good homogeneity. The melt was rapidly quenched in cold water from 800 K and the cooling rate was estimated to be 200 K s^{-1}. The ingots obtained by quenching were cut into sheets with mirror-like surfaces of about 50–200 μm thickness. The composition of the samples was measured by electron probe microanalysis. X-ray diffraction patterns did not contain any peaks owing to crystallinity.

2.2. Experimental set-up

The experimental apparatus used for recording TSD currents is classical [6, 7]; it is essentially composed of a sample holder, stabilized voltage supply and a current detector.

The samples for the TSD measurements were mounted in an evacuated ($P \simeq 10^{-3}$ Pa) cryostat on a holder cooled with liquid nitrogen and heated with a resistance heater. The temperature was measured with thoroughly calibrated copper–constantan thermocouples. The sample was provided with a digitally controlled voltage supply of extreme stability and low noise level. The current was measured with an electrometer.

In the TSD experiment considered here, a sample is cooled to a low temperature (about 100 K) and photoexcited for a time $t_p (\simeq 4$ *min*) in the presence of an applied DC field ($E = 3 \times 10^4$ V cm^{-1}). Then the light and voltage are switched off and after a delay period, necessary for sample relaxation (to reach equilibrium between the free and the trapped carriers), the sample is heated in darkness at a constant rate β while the TSD is measured.

3. Results

3.1. Thermally stimulated depolarization in pure selenium

The TSD experiments on glassy selenium samples start from the 'photolectret' state. Because the photopolarization processes are most strongly expressed at blocking electrodes an in order to separate the TSD peak from the DC conduction, we placed a highly insulating layer between the glass specimen and the metal electrodes in the measuring cell. Two different materials were used as the dielectric insulator: cleaved mica sheet and Teflon. The two dielectric materials gave essentially the same results.

TSD measurements on glassy selenium samples display a well shaped peak at $T_m = 150$ K. At lower heating rates β, the peak shifts to lower temperatures and is reduced in height, as expected (figure 1). The activation energy E_i associated with the peak at $T_m = 150$ K has been calculated by the initial rise method [16], i.e. plotting $\log I$ against $1/T$ from the initial rise of the curves. Such a plot for $\beta = 0.08$ K s^{-1} is shown in the inset. The activation energy obtained by this method is 0.22 eV. An independent check of the correctness of the activation energy E_i can be obtained by measuring the TSD at different heating rates β. A plot of $\ln(T_m^2/\beta)$ against $1/T_m$ yields a straight line [17, 18], from the slope of which the activation energy is 0.24 eV. The latter value of E_i is consistent with that estimated from the initial rise method. Our results on TSD measurements on pure Se

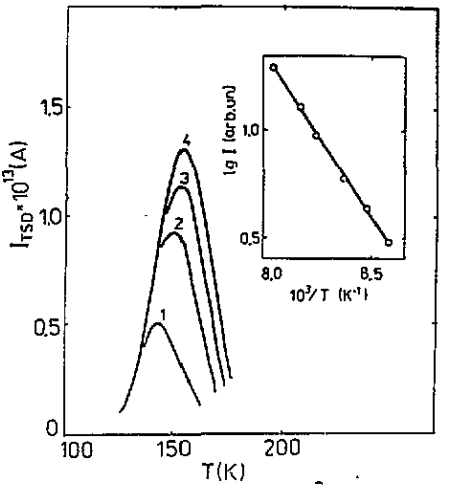

Figure 1. Variation in the TSD for various heating rates β in pure amorphous selenium: curve 1, 0.08 K s^{-1}; curve 2, 0.17 K s^{-1}; curve 3, 0.23 K s^{-1}; curve 4, 0.44 K s^{-1}. The inset shows the Arrhenius plot of TSD for curve 1.

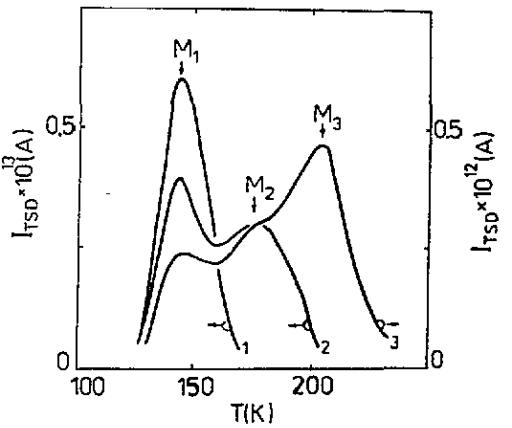

Figure 2. TSD spectra of Sb_xSe_{1-x} alloys: curves 1, $x = 0$; curve 2, $x = 0.01$; curve 3, $x = 0.05$.

are in relatively good agreement with previously reported data [8, 19, 20] on the gap-states profile.

It is necessary to note that the systematic variation in specimen thickness (between 50 and 500 μm) and those of different materials as the dielectric insulator yielded nearly the same peak position and activation energy. This suggests strongly that disturbing contact effects were absent. Moreover, no difference was observed between specimens which were open circuited or short circuited during cooling, nor did the time interval between irradiation and subsequent heating appear to have any effect on the observations. Therefore, it appears that the TSD currents considered here are the true TSD currents associated with thermal release of non-equilibrium carriers from localized gap states. The trap of activation energy 0.22–0.24 eV acts as a shallow trap.

3.2. TSD in Sb_xSe_{1-x} alloys

For TSD in Sb_xSe_{1-x} alloys, we have three peaks M_1, M_2 and M_3 whose maximum temperatures T_{M_1}, T_{M_2} and T_{M_3} (145 K, 175 K and 195 K, respectively) are close enough to each other that they overlap (figure 2). In order to separate and isolate these peaks from each other, the so-called 'thermal cleaning' method [21, 22] was used. After the whole curve has been obtained, a second thermal cycle is started but we first discharge the lower-temperature peak M_1 by heating until T_a ($T_{M_1} < T_a < T_{M_2}$), then cool the sample again and finally obtain the discharge of peak M_2, which is nearly pure. Peak M_3 can also be isolated in a similar way by using $T_b > T_{M_2}$. Figure 3 shows the results obtained by such step heating. Three peaks are separated by thermal cleaning. The activation energy was conventionally determined as $E_{i1} = 0.22$ eV, $E_{i2} = 0.34$ eV and $E_{i3} = 0.45$ eV, using the initial rise method.

Another modification of the thermal cleaning method consists of first polarizing the material at a temperature T_p such that $T_{M_1} < T_p < T_{M_2}$ (the traps of type M_2 and M_3 are filled, while the traps of type M_1 remain almost empty). The resulting TSD curve then

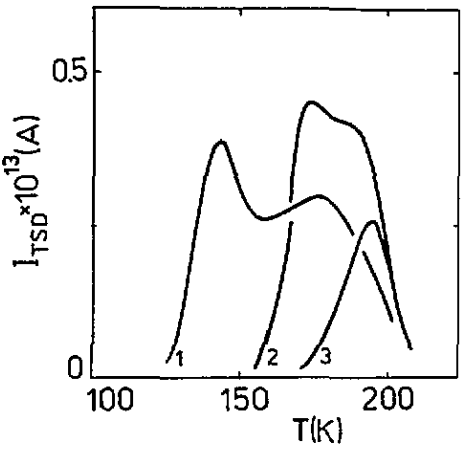

Figure 3. Thermal cleaning procedure of the TSD in $Sb_{0.01}Se_{0.99}$. $T_a = 165$ K and $T_b = 195$ K (see the text).

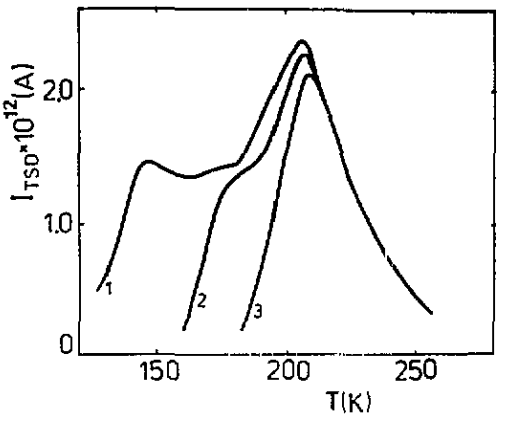

Figure 4. The TSD peaks isolated by photopolarizing the $Sb_{0.05}Se_{0.95}$ sample at $T_p = 90$ K (curve 1), 169 K (curve 2) and 184 K (curve 3).

shows only peaks M_2 and M_3. The polarization current obtained for samples polarized at $T_{M_2} < T_p < T_{M_3}$ gives a pure (single) maximum M_3. Such an effective way of separating the above-mentioned peaks is illustrated in figure 4. Note that there was no significant difference between the activation energies E_i deduced from the corresponding TSD curves shown in figures 3 and 4.

The technique used here gives useful information about the distribution of the density of states. In fact, inspection of the thermally stimulated current (initial rise in step-heating procedure) indicates that the gap states in pure selenium are relatively discrete (ΔE for M_1 is about 0.02 eV or less) while in Sb_xSe_{1-x} they are distributed in energy ($\Delta E = 0.04$–0.06 eV for M_2 and M_3).

3.3. Determination of the type of carrier trap

Independent evidence for defect states and the charge of the trapped carriers comes from time-of-flight measurements [23]. Current transient waveforms were observed and the mobility μ was obtained from the well defined transit time t_T according to the equation $\mu = L/Et_T$, where L is the thickness of the sample and E is the applied electric field.

The effect on the room-temperature transit pulse shapes of Sb addition to Se is illustrated in figure 5. Note that in Sb_xSe_{1-x} it was not possible to detect any pulses associated with the transit of hole carriers. Only lifetime-limited signals were observed for the case of photoinjected holes. For these signals the transit time cannot be extracted by using even a double-logarithmic representation.

The effect of Sb on electron transport is less spectacular. Although Sb alloying increases the transit time dispersion, the transit shown contains a clearly identifiable break in the waveform.

At room temperature, the transit time scales linearly with the sample thickness as is expected [24, 25] for transient transport with Gaussian dispersion.

The shape of the transient current for Sb_xSe_{1-x} is remarkably unstable with respect to temperature (figure 6). In analogy with the behaviour observed for pure Se [26], electron traces for Sb_xSe_{1-x} show a progressive increase in dispersion as the temperature is lowered.

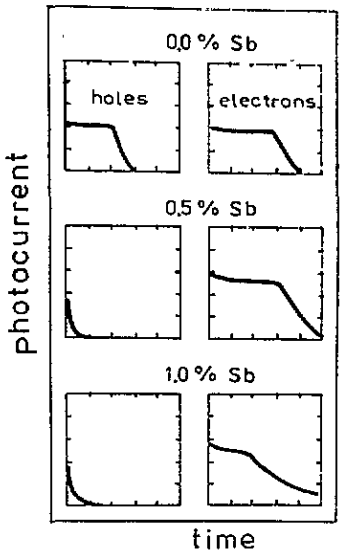

Figure 5. Comparison of room-temperature transit pulse shapes in amorphous selenium alloyed with Sb. For Se, $E = 8.0\times10^6$ V m^{-1} and 0.1 μs per division for holes and 2 μs per division for electrons. For 0.5 at.% Sb, $E = 9.0 \times 10^6$ V m^{-1} and 0.1 μs per division for holes and 2 μs per division for electrons. For 1 at.% Sb, $E = 8.8 \times 10^6$ V m^{-1} and 0.1 μs per division for holes and 5 μs per division for electrons.

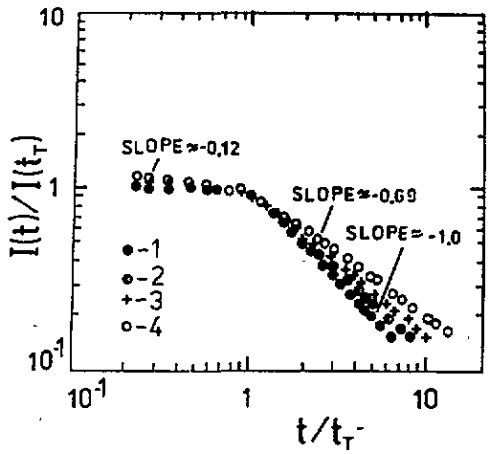

Figure 6. Temperature dependence of transient electron current shape in amorphous $Sb_{0.01}Se_{0.99}$ at 8.8×10^6 V m^{-1} for: ●, $T = 293$ K, ○, 278 K, +, 269 K and ○, 259 K.

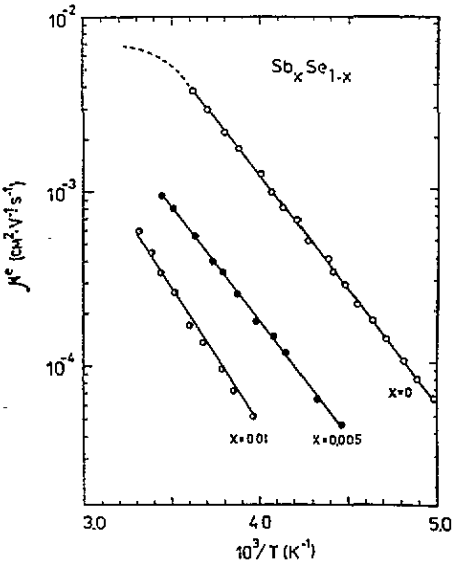

Figure 7. Temperature dependence of electron drift mobility in amorphous Sb_xSe_{1-x}.

Transit pulses observed in Sb_xSe_{1-x} films may be characterized to first order as involving two power-law regimes:

$$I_1 \sim t^{-(1-\alpha_1)} \qquad (0 < t < t_T)$$

$$I_2 \sim t^{-(1+\alpha_2)} \qquad (t > t_T).$$

The estimated values of α_1 and α_2 are not equal to each other. As can be seen from figure 6,

the values of α_2 exhibit a much more rapid temperature dependence than those of α_1. It becomes clear from the examination of phototransients that universality of the pulse shape (predicted by a stochastic transport model [24]) with respect to temperature is not observed in our case. The qualitative observation is that small signal transients become increasingly dispersive as the sample temperature is reduced.

The electron drift mobility in Sb_xSe_{1-x} alloys exhibits Arrhenius behaviour (figure 7). The experimentally observed activation energy of Se, namely $E_\mu = 0.33$ eV (note that E_μ actually corresponds to one of the traps detected by TSD, i.e. E_{t2}), remains almost insensitive to Sb addition in the range investigated. At the same time, the mobility decreases with increasing Sb content.

It is reasonable, within the framework of a shallow-trap-controlled mobility model [27], to interpret our time-of-flight observations in the following manner. In pure Se, electron transport is controlled by a narrow manifold of traps located about 0.33 eV from the conduction band mobility edge. The transport tends to become dispersive when kT is less than the nominal trap manifold width ΔE. Note here that, in the simulation studies of Marshall [25], various distributions of trapping centres were examined and it was established that, in each case, highly dispersive transit pulses could be generated if the localized states extended over more than a few kT. A distribution of the Gaussian form is capable of generating values of α_1 and α_2 with a temperature dependence similar to that of typical experimental data for Se. The addition of Sb to Se, as we believe, broadens the distribution of shallow traps, thus shifting the threshold for non-dispersive transport to higher temperatures. The decrease in electron mobility with increasing Sb content can be accounted for by the increase in the density of shallow traps with E_μ remaining constant at approximately 0.33 eV, or, alternatively, by the appearance of additional shallow traps located close to that in Se.

Unlike the electron case, the effect of Sb on hole transport cannot be explained by a gradual change in the density and energy distribution of shallow traps. We can attribute the lifetime-limited hole signal to the loss of carriers from the photoinjected charge packet due to deep trapping. It is interesting to note that similar behaviour in hole drift mobility was observed [27, 28] in the As–Se system in the concentration range 2–6 at.% As.

We conclude from the drift mobility measurements that the addition of Sb to Se increases the integrated number of deep traps (decreases the photoinjected hole range) and shallow traps (decreases the electron drift mobility). Additionally, one might expect a concomitant disorder-induced (compositional as well as structural) broadening in the distribution of shallow gap states.

Since the time-of-flight measurements show that the mobile carriers in Sb_xSe_{1-x} alloys are negative electrons in the Sb concentration range $0 < x \leqslant 0.05$, the above trapping centres manifested in TSD are most likely to act as electron traps.

4. Conclusion

The results taken as a whole reveal the existence of at least three main different trap species in Sb_xSe_{1-x} non-crystalline semiconductors. These species are located at energies 0.22, 0.34 and 0.45 eV, respectively, below the conduction band edge and control the electron transport properties of the material. It seemed that Sb introduces a new set of detectable electron traps.

Acknowledgments

We gratefully acknowledge the technical assistance of Dr A R Levkulich, Dr A V Mateleshko and Dr P P Shtets.

References

[1] Madan A and Shaw M P 1988 *The Physics and Applications of Amorphous Semiconductors* (New York: Academic)
[2] Spear W E 1988 *Proc. R. Soc.* A **420** 201
[3] Mott N F and Davis E A 1982 *Electron Processes in Non-Crystalline Materials* 2nd edn (Moscow: Mir) (Russian translation)
[4] Pirogov F V 1989 *J. Non-Cryst. Solids* **114** 76
[5] Pirogov F V and Shvarts K K 1987 *J. Non-Cryst. Solids* **97–8** 1211
[6] Braunlich P, Kelly P and Fillard J P 1979 *Thermally Stimulated Relaxation in Solids (Top. Appl. Phys. 37)* ed P Braunlich (Berlin: Springer) p 35
[7] Gorokhovatasky Yu and Bordovskij G 1991 *Thermally Activational Current Spectroscopy of High-Resistance Semiconductors and Dielectrics* (Moscow: Nauka)
[8] Street R A and Yoffe A D 1972 *Thin Solid Films* **11** 161
[9] Kolomiets B T, Lyubin V M and Averjanov V L 1970 *Mater. Res. Bull.* **5** 655
[10] Botila T and Henish H K 1976 *Phys. Status Solidi* a **36** 331
[11] Agarwal S C 1974 *Phys. Rev.* B **10** 4340
[12] Agarwal S C and Fritzsche H 1974 *Phys. Rev.* B **10** 4351
[13] Muller P 1981 *Phys. Status Solidi* a **67** 11
[14] Kikineshi A A, Mikla V I and Mikhalko I P 1977 *Sov. Phys.–Semicond.* **11** 1010
[15] Mikla V I 1984 *PhD Thesis* Odessa State University
[16] Garlick G F and Gibson A F 1948 *Proc. Phys. Soc.* **60** 574
[17] Bohun A 1954 *Czech. J. Phys.* **4** 91
[18] Bohun A H 1954 *Can. J. Chem.* **32** 214
[19] Kang T W, Tong C, Leem J Y and Kim T W 1991 *J. Appl. Phys.* **69** 3115
[20] Owen A E and Spear W E 1976 *Phys. Chem. Glasses* **117** 174
[21] Perlman M M and Unger S 1974 *J. Appl. Phys.* **69** 3115
[22] Bucci C, Frieschi R and Guidi G 1966 *Phys. Rev.* **152** 833
[23] Spear W E 1969 *J. Non-Cryst. Solids* **1** 197
[24] Scher H and Montroll E 1975 *Phys. Rev.* B **12** 2455
[25] Maishall J M 1983 *Rep. Prog. Phys.* **46** 1235
[26] Pfister G 1976 *Phys. Rev. Lett.* **36** 271
[27] Marshall J M, Fisher F D and Owen A E 1974 *Phys. Status Solidi* a **25** 419
[28] Schottmiller J, Tabak M, Lucovsky G and Ward A 1970 *J. Non-Cryst. Solids* **4** 80